



**HAL**  
open science

# Alpha clustering and nuclear molecules in $8\text{ Be}$ , $12\text{ C}$ , $16\text{ O}$ , $20\text{ Ne}$ , $24\text{ Mg}$ , and $32\text{ S}$

Guy Royer, Philippe Eudes

► **To cite this version:**

Guy Royer, Philippe Eudes. Alpha clustering and nuclear molecules in  $8\text{ Be}$ ,  $12\text{ C}$ ,  $16\text{ O}$ ,  $20\text{ Ne}$ ,  $24\text{ Mg}$ , and  $32\text{ S}$ . 11th International Conference on Clustering Aspects of Nuclear Structure and Dynamics, University of Napoli Italy, May 2016, Napoli, Italy. pp.012012, 10.1088/1742-6596/863/1/012012 . hal-01557468

**HAL Id: hal-01557468**

**<https://hal.science/hal-01557468>**

Submitted on 6 Jul 2017

**HAL** is a multi-disciplinary open access archive for the deposit and dissemination of scientific research documents, whether they are published or not. The documents may come from teaching and research institutions in France or abroad, or from public or private research centers.

L'archive ouverte pluridisciplinaire **HAL**, est destinée au dépôt et à la diffusion de documents scientifiques de niveau recherche, publiés ou non, émanant des établissements d'enseignement et de recherche français ou étrangers, des laboratoires publics ou privés.



Distributed under a Creative Commons Attribution 4.0 International License

# Alpha clustering and nuclear molecules in ${}^8\text{Be}$ , ${}^{12}\text{C}$ , ${}^{16}\text{O}$ , ${}^{20}\text{Ne}$ , ${}^{24}\text{Mg}$ , and ${}^{32}\text{S}$

**G. Royer, P. Eudes**

Subatech, Université-IN2P3/CNRS-Ecole des Mines, 44307 Nantes, France

E-mail: royer@subatech.in2p3.fr

**Abstract.** Within a liquid drop model the energy of the  ${}^{12}\text{C}$ ,  ${}^{16}\text{O}$ ,  ${}^{20}\text{Ne}$ ,  ${}^{24}\text{Mg}$  and  ${}^{32}\text{S}$  4n-nuclei has been calculated within different configurations of  $\alpha$ -molecules : linear chain, triangle, square, tetrahedron, pentagon, trigonal bipyramid, square pyramid, hexagon, octahedron, octagon and cube. The potential barriers governing the decay and entrance channels via  $\alpha$  emission or absorption as well as the potential barriers of other possible binary and ternary reactions have been compared. The rms radii of the linear chains do not correspond to the experimental rms radii of the ground states. The binding energies of the three-dimensional molecules at the nascent point of the fragments are higher than the ones of the planar configurations. The A-4 daughter plus  $\alpha$  particle configurations have always the lowest potential energy.

## 1. Introduction

Hydrogen burning in stars leads to a core of helium and, later on, to the nucleosynthesis of n- $\alpha$  nuclei :  ${}^{16}\text{O}$ ,  ${}^{20}\text{Ne}$ ,  ${}^{24}\text{Mg}$ ,  ${}^{28}\text{Si}$ ,  ${}^{32}\text{S}$ , ... The cluster-type states coexist with the mean-field-type states [1] in these specific nuclei. In  ${}^{12}\text{C}$  a large amount of  $3\alpha$  cluster wave function is contained in the ground state wave function. Recently, a new high spin  $5^-$  state has been observed. It corresponds to a level of the ground state rotational band of an equilateral triangular spinning top [2]. In  ${}^{16}\text{O}$ , recent studies lead, for the ground state, to a tetrahedral configuration allowing to reproduce the energy spectrum and the electromagnetic properties [3, 4]. Some excited states are due to the mean-field-type excitation mode while other ones are due to the cluster structure of  $\alpha+{}^{12}\text{C}$ . For the excited  $0_2^+$  Hoyle state of  ${}^{12}\text{C}$  and possible excited Hoyle state of  ${}^{16}\text{O}$ , the  $\alpha$  condensate character chain has been proposed after comparing a large number of Brink functions with Tohsaki-Horiuchi-Schuck-Röpke wave functions [5, 6].

The generalized liquid drop model (GLDM) describing correctly the fusion [7], alpha emission [8] and fission [9] processes has been used to calculate the L-dependent potential energy of the following  $\alpha$  clusters: aligned  $\alpha$  chains, isosceles triangle, square, tetrahedron, pentagon, trigonal bipyramid, square pyramid, hexagon, octahedron, octagon and cube [10, 11]. The proximity energy is included in this model to take into account the effects of the nuclear forces between the surfaces in regard in a gap or a neck between nuclei.

## 2. ${}^{12}\text{C}$ nucleus

Antisymmetrized Molecular Dynamics and Fermionic Molecular Dynamics models without assuming  $\alpha$  clustering led naturally for the different states to triangular  $\alpha$  shapes with different

angles allowing the reproduction of the low-lying spectrum [12, 13]. Within effective field theory and Monte Carlo lattice calculations it has been demonstrated that the  $^{12}\text{C}$  ground state has a compact triangular configuration while the Hoyle state and the second excited state have rather an obtuse triangular shape of alpha particles [14]. These predictions are strengthened by the observation of the high spin  $5^-$  state at 22.4 MeV.

These oblate ternary configurations have been investigated within the GLDM and an isosceles triangular shape characterized by an angle  $\theta$ . At the contact point the energy of the linear chain of three  $\alpha$  particles ( $\theta=180$  deg.) is higher than the energy of the equilateral triangular shape, the difference being 7.4 MeV. This is also in favor of the equilateral triangular configuration (the energy being degenerated between 120 and 180 degrees). The experimental rms charge radius of the ground state is  $\langle r^2 \rangle^{1/2} = 2.47$  fm while, within the GLDM, the rms radius of the triangular shape is 2.43 fm and 3.16 fm for a linear chain at the contact point [10].

### 3. $^{16}\text{O}$ nucleus

A tetrahedral molecule of alpha particles is predicted for the ground state [3, 4] and a square

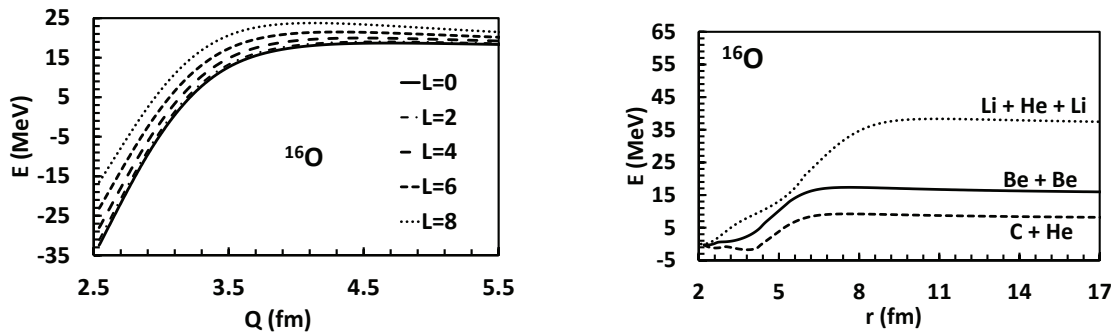


**Figure 1.** Potential energy of the  $\alpha$ -tetrahedron (left part) as functions of the angular momentum (in  $\hbar$  unit) and rms radius and (right part) potential energy governing the  $^{12}\text{C}+^4\text{He}$ ,  $^8\text{Be}+^8\text{Be}$ , and  $^6\text{Li}+^4\text{He}+^6\text{Li}$  nuclear systems versus the distance between the mass centres.

configuration for the first excited spin-0 state. The energies of the tetrahedral shape are given in Fig. 1. The rms radius is 2.54 fm for a tetrahedron, 2.83 fm for a square and 4.15 fm for a prolate linear chain at the contact point between the four  $\alpha$  particles. Experimentally the rms charge radius of the ground state is  $\langle r^2 \rangle^{1/2} = 2.70$  fm excluding probably a linear chain configuration for the ground state. The binding energy is higher for the tetrahedral molecule than for the square shape since for these molecular shapes the proximity energy plays a crucial role. Indeed, the tetrahedron is linked by six bonds and the square by only four bonds. On the contrary, the Coulomb repulsion is higher for the tetrahedral shape. The energy difference between the two configurations is 13.7 MeV close to the  $Q_{4\alpha}$  (14.4 MeV), the energy of the  $0_6^+$  state (15.1 MeV) and 14.0 MeV the energy of a  $0^+$  state.

The ground state may also be described using double closed shell wave functions but several excited states may also be viewed within the  $^{12}\text{C}+^4\text{He}$  cluster picture. The potential energies of the  $^{12}\text{C}+^4\text{He}$ ,  $^8\text{Be}+^8\text{Be}$ , and aligned  $^6\text{Li}+^4\text{He}+^6\text{Li}$  systems have been determined assuming a spherical shape for all nuclei (see Fig. 1). The top of the barriers corresponds to separated nuclei maintained in unstable equilibrium. Quasimolecular  $^{12}\text{C}+^4\text{He}$  one-body shapes with a deep neck have roughly the same energy than the spherical compound nucleus.

#### 4. $^{20}\text{Ne}$ nucleus

The trigonal bipyramid, square pyramid and pentagonal molecular configurations have been compared. Their energies are displayed in Fig. 2. The rms radius is 2.76 fm for a trigonal bipyramid, 2.79 fm for a square pyramid and 3.29 fm for a pentagon. The experimental rms charge radius is  $\langle r^2 \rangle^{1/2} = 3.01$  fm, much lower than the rms radius of a prolate chain. The binding energy of the trigonal bipyramid is the highest since the number of bonds is five for the pentagon, eight for the square pyramid and nine for the trigonal bipyramid. At the contact point, the energy difference between the trigonal bipyramid and the square pyramid is 21.3 MeV and 15.3 between the square pyramid and the pentagon, the  $Q_{5\alpha}$  value being 19.2 MeV.

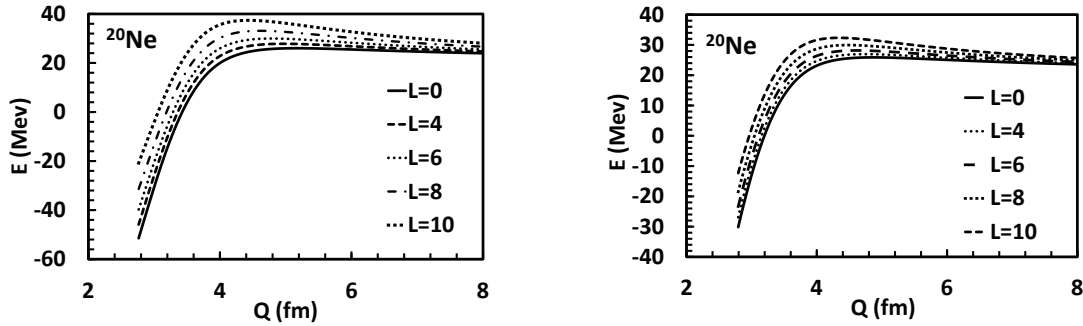


**Figure 2.** Potential energy of the trigonal bipyramid (on the left) and the square pyramid (on the right) as functions of the angular momentum and rms radius.

The ground state band contains the  $^{16}\text{O}+^4\text{He}$  cluster at most 70% and the potential energies of the  $^{16}\text{O}+^4\text{He}$ ,  $^{12}\text{C}+^8\text{Be}$ ,  $^{10}\text{B}+^{10}\text{B}$ , and linear  $^8\text{Be}+^4\text{He}+^8\text{Be}$  systems have been determined. In the  $^{16}\text{O}+^4\text{He}$  channel quasimolecular one-body shapes have roughly the same energy than the spherical nucleus and the minimum has a cluster structure corresponding to the two  $^4\text{He}$  and  $^{16}\text{O}$  nuclei almost in contact.

#### 5. $^{24}\text{Mg}$ nucleus

The energies of the octahedral and hexagonal  $\alpha$ -molecules are shown in Fig. 3. The experimental rms charge radius of the ground state is only  $\langle r^2 \rangle^{1/2} = 3.06$  fm. At the contact point the rms radius is 2.85 fm for an octahedron and 3.79 fm for an hexagon excluding the linear chain and planar shape as possible ground state shapes. The binding energy is lower for the hexagonal configuration since there are only six bonds for the hexagon and twelve for the octahedron.

The energies of the  $^{16}\text{O}+^8\text{Be}$ ,  $^{12}\text{C}+^{12}\text{C}$ ,  $^8\text{Be}+^8\text{Be}+^8\text{Be}$ , and  $^{10}\text{B}+^4\text{He}+^{10}\text{B}$  systems are shown in Fig. 3.

#### 6. $^{32}\text{S}$ nucleus

The octagonal and cubic  $\alpha$ -configurations have been studied. The experimental rms charge radius is  $\langle r^2 \rangle^{1/2} = 3.26$  fm while the rms radius is 4.85 fm for an octagon and 3.37 fm for a cube at the contact point which seems to exclude the planar and linear configurations. The binding energy is higher for the cubic configuration than for the octagonal shape since there are twelve bonds for the cube and only eight for the octagon.

The potential energies of the  $^{28}\text{Si}+^4\text{He}$ ,  $^{24}\text{Mg}+^8\text{Be}$ ,  $^{20}\text{Ne}+^{12}\text{C}$ , and  $^{16}\text{O}+^{16}\text{O}$  systems have been also determined. The energy of the one-body  $^{28}\text{Si}+^4\text{He}$  system is relatively constant from

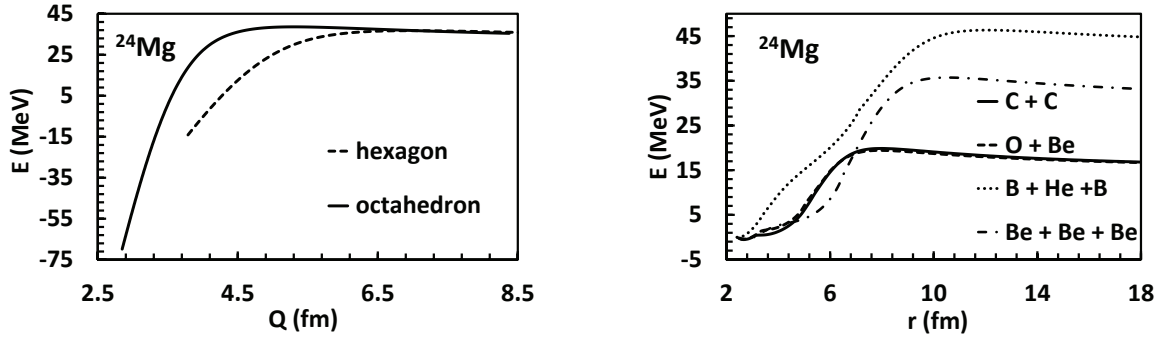


**Figure 3.** Potential energies of an hexagon and an octahedron from the contact point as a function of the rms radius and potential barriers governing the  $^{16}\text{O}+^8\text{Be}$ ,  $^{12}\text{C}+^{12}\text{C}$ ,  $^8\text{Be}+^8\text{Be}+^8\text{Be}$ , and  $^{10}\text{B}+^4\text{He}+^{10}\text{B}$  reactions versus the distance between the mass centres.

the spherical nucleus till the contact point allowing the cohabitation of different quasimolecular shapes.

## 7. Conclusion

Within an  $\alpha$ -particle model the energy of the  $^{12}\text{C}$ ,  $^{16}\text{O}$ ,  $^{20}\text{Ne}$ ,  $^{24}\text{Mg}$  and  $^{32}\text{S}$  nuclei has been calculated within different  $\alpha$ -molecular configurations: linear chain, triangle, square, tetrahedron, pentagon, trigonal bipyramid, square pyramid, hexagon, octahedron, octagon, and cube. Within a macroscopic approach the potential barriers governing the entrance and decay channels of these  $4n$ -nuclei via alpha absorption or emission and other possible nuclear systems have also been compared.

The rms radii of the prolate chains seem incompatible with the experimental rms radii of the ground states. The binding energies of the three-dimensional molecules are higher than the binding energies of the planar shapes. The core+ $\alpha$  cluster system leads always to the lowest potential barrier.

## References

- [1] von Oertzen W, Freer M, and Kanada-En'yo Y 2006 *Phys. Rep.* **432** 43
- [2] Marin-Lambarri D J *et al.* 2014 *Phys. Rev. Lett.* **113** 012502
- [3] Epelbaum E *et al.* 2014 *Phys. Rev. Lett.* **112** 102501
- [4] Bijker R and Iachello F 2014 *Phys. Rev. Lett.* **112** 152501
- [5] Funaki Y *et al.* 2009 *Phys. Rev. C* **80** 064326
- [6] Suhara T, Funaki Y, Zhou B, Horiuchi H, and Tohsaki A 2014 *Phys. Rev. Lett.* **112** 062501
- [7] Royer G, Remaud B 1985 *Nucl. Phys. A* **444** 477
- [8] Royer G 2010 *Nucl. Phys. A* **848** 279
- [9] Royer G, Jaffré M, and Moreau D 2012 *Phys. Rev. C* **86** 044326
- [10] Royer G, Escudie A, and Sublard B 2014 *Phys. Rev. C* **90** 024607
- [11] Royer G, Ramasamy G, and Eudes P 2015 *Phys. Rev. C* **92** 054308
- [12] Kanada-En'yo Y 2007 *Prog. Theor. Phys.* **117** 655
- [13] Chernykh M *et al.* 2007 *Phys. Rev. Lett.* **98** 032501
- [14] Epelbaum E *et al.* 2012 *Phys. Rev. Lett.* **109** 252501